In Silico Analysis of Phytoconstituents against Major Psoriatic and Inflammatory Target Proteins

Sagar N. Ande*, Mahendra D. Kshirsagar, Anil V. Chanderwar, Nitin I. Kochar, Deepak S. Mohale

Department of Pharmacology and Toxicology, P. Wadhwani College of Pharmacy, Yavatmal, Maharashtra, India

Address for Correspondence:

Name of the Author: Sagar N. Ande,

Department Name: Department of Pharmacology and Toxicology

Institute Name: P. Wadhwani College of Pharmacy,

Institute Address: Yavatmal - 445 001, Maharashtra, India.

E-mail: sagar986ande@gmail.com

Running Title: Analysis of *In Silico* Phytoconstituents against Inflammatory Target Proteins

ABSTRACT

In silico screening of phytochemicals active constituents performs for anti-psoriatic and anti-inflammatory properties to treat psoriasis. A chronic inflammatory skin condition with significant hereditary tendency and autoimmune pathologic characteristics is psoriasis. The frequency varies by area but is roughly 2% globally people affected by this disease. The interleukin (IL)-23/Th17 and IL-17 axis is a major contributing factor in psoriatic disease. For the purpose of examining the interactions of active substances with specific proteins, Autodock 4.2 was used to screen potential constituents. High protein binding affinities and low inhibition constants were used to determine which ligands had the best affinity for proteins. Biovia Discovey Software was used to monitor the ligands' binding spaces, hydrogen bonds, and hydrophobic bonds.

Key words: ***In Silico* , Phytoconstituents** , **Target Proteins**

INTRODUCTION

Psoriasis vulgaris is the most well-known and accessible human disease mediated by T lymphocytes and dendritic cells. Inflammatory myeloid dendritic cells secrete Interleukin (IL)-23 and IL-12, which stimulate IL-17-producing T cells, Th1 cells, and Th22 cells, resulting in an abundance of psoriatic cytokines such as IL-17, interferon, tumor necrosis factor (TNF), and IL-22. These cytokines act on keratinocytes to increase psoriatic inflammation and investigations have revealed the role of the major cytokines IL-23, TNF, Cyclooxygenase-2 (COX-2), and IL-17 in this process.(Anand & Kaithwas. 2014 ; Gudjonsson et al. 2004; Kamiy et al. 2019)

About 75–80% of the world's population still relies heavily on herbal therapy, particularly in developing nations as for primary healthcare since they are more socially acceptable, more compatible with human bodies, and have less toxicity.(Qazi et al.2021) The chemical components of phytochemicals are believed to be more compatible with the human body because they are a part of the physiological processes of living flora.

In this course of work, docking studies by AutoDock4.2 were used to conduct virtual screening, which provides a concept of the most efficient and physiologically appropriate herbal molecule for drug receptor interaction.(Rauf et al. 2015). The most vital stage of drug development studies is virtual screening. Molecular docking is a new rational approach in drug design method where it is anticipated that a small molecule is certain to exhibit affinity and experimentally bind to the binding site of the target receptor. To estimate the affinity and activity of the chosen molecule with the target protein, docking is widely used to predict the binding orientation of any small molecule or drug candidates to their protein targets. Undoubtedly docking has a significant impact on the pharmaceutical sector. (Sharmila 2019)

METHODOLOGY

AutoDock 4.2.6 is an automated approach for predicting ligand interactions with biomacromolecular targets to compute ligand binding affinity and inhibition constants towards proteins. We used 10 phytochemical to screen against four target proteins. Two of the four proteins are psoriasis targets (IL-17 and IL-23) and two are inflammatory targets (COX-2 and TNF-α). The phytochemical are *Coleus forskohlii*, *Rubia cordifolia*, *Azadirachta indica*, *Boswellia serrata*, *Curcuma longa*, *Glycyrrhiza glabra*, *Aloe barbadensis*, White willow bark, *Berberis aristata*, and *Lagerstroemia speciosa*. At first, it was checked for maximum contributing active components from the all extracts before proceeding for

docking.

Ligand preparation

All the active components structure details were derived from chembank and drug bank. Those structure was prepared for docking purpose using autodock itself or using biovia discovery studio software with following steps:

1. Add hydrogen atoms to the molecule
2. Add partial charges (Kollman)
3. Delete non-polar hydrogen's and merge their charges with the carbon atoms
4. Assign atom types, defining hydrogen bond acceptors and donors and aromatic and aliphaticcarbon atoms
5. Choose a root atom that will act as the root for the torsion tree description of flexibility
6. Define rotatable bonds and build the torsion tree.

Then, read the molecule into AutoDockTools using the Ligand (for the ligand) or Grid (forThe receptor) menus, and create the PDBQT file.

Protein preparation

All proteins structure was extracted from PDB databases(IL-17: PDB id-3JVF, IL-23: PDB id-3DUH, COX-2: PDB id-1CX2, TNF-α: PDB id-1TNF) and prepared for docking purpose using previously mentioned steps. Then saved the files using PDBQT format.

Grid box preparation

As autodock required pre-calculated grid map file for docking calculation very fast, grid box was prepared for whole protein (unknown Binding cavity) so it covered all binding possibilities of ligands with proteins. The grid file was saved as **.**gpf format. Using the Centre Grid Box field, which moves the Grid Box along the X, Y, and Z axes, the position of the Grid Box can be changed to cover the binding site or binding residues.

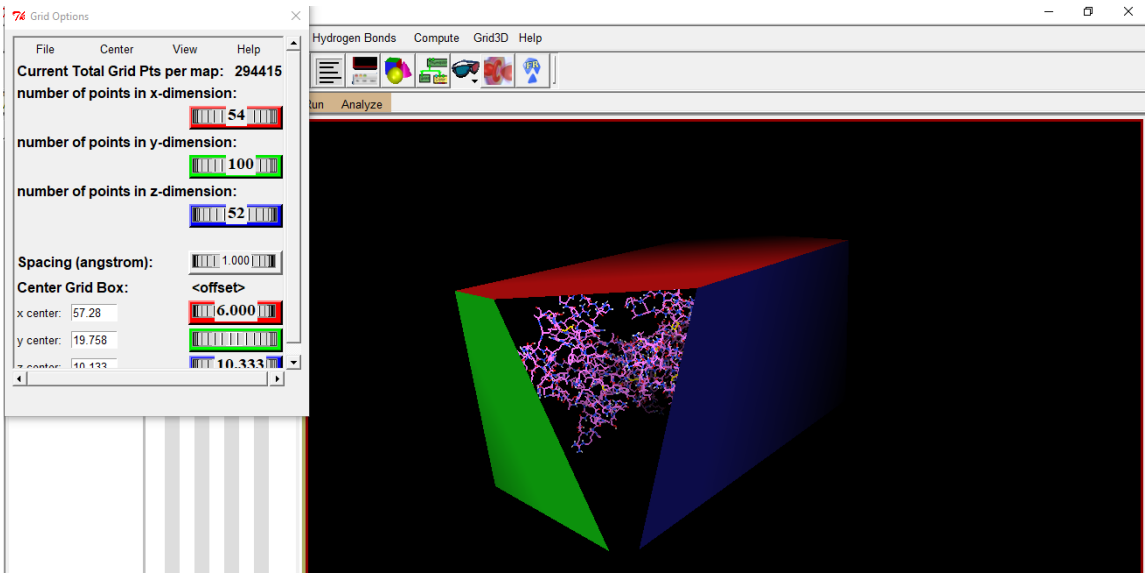

Executive autogrid 4

To specify the region or area of the protein to be examined for the interaction with the ligand molecule, AutoGrid must be run, which required grid parameter file (gpf) to specify the files and parameters used in the calculation. Output of the auto grid generated as **.glg** format (grid log file).After AutoGrid has been successfully finished, AutoDock can be run. The interactions between the ligand molecule and the amino acid inside the Grid Box are computed by AutoDock.

1tnf.A.map	MAP File	2'293 KB
1tnf.Br.map	MAP File	2'328 KB
1tnf.C.map	MAP File	2'297 KB
1tnf.Cl.map	MAP File	2'312 KB
1tnf.d.map	MAP File	2'055 KB
1tnf.e.map	MAP File	3'040 KB
1tnf.F.map	MAP File	2'255 KB
1tnf.HD.map	MAP File	2'156 KB
1tnf.maps.fld	FLD File	3 KB
1tnf.maps.xyz	XYZ File	1 KB
1tnf.N.map	MAP File	2'284 KB
1tnf.NA.map	MAP File	2'284 KB
1tnf.OA.map	MAP File	2'277 KB
1tnf.pdbqt	PDBQT File	344 KB
1tnf.SA.map	MAP File	2'308 KB

Docking with autodock

AutoDock offers a number of ways to carry out the conformation search. The Lamarckian Genetic Algorithm currently offers the most effective search for general applications and will be employed in the majority of cases. (Prasanth et al. 2021). When compared to the various search techniques in AutoDock4.2 for ligand conformational searching, the Lamarckian genetic algorithm performs better than simulated annealing or the simple genetic algorithm.

The approach makes use of a five-term force field-based function that was generated from the AMBER force field include different descriptor like Lennard-Jones dispersion term, a directional hydrogen bonding term, a coulombic electrostatic potential term, and an entropic term.(Saxena et al. 2021.a; Saxena et al. 202.b) The same algorithm was employed by us for both screening and autodock operations. The **.dpf** file is essential since it contains details about all parameters and map files. The docking parameter file instructs AutoDock as to which grid map files to use, which ligand molecule to dock, as to what its center and number of torsions are, as to where to start the ligand, as to which flexible residues to move to model side chain motion in the receptor, as well as which docking algorithm to use and how many runs to perform. The output of the docking process was produced in **.dlg** format.

Analyzing dock results

The initial step in examining the outcomes of docking experiments is reading a docking log or set of docking logs. The docked structures discovered at the end of each run, their energies, and the conformational clustering analysis are the most crucial components of a docking log file. A graphical user interface for Autodock were used to analyze the docking log (dlg) files. The root mean square deviation tolerance for the final docked conformations was under 2A.(Sravani et al. 2021) Based on the binding energy, each ligand's docked conformations were grouped into clusters. Visual analysis of the top-ranked conformations was conducted using Biovia discovery studio and cross checked with Ligplot and proteinplus.

RESULTS AND DISCUSSION

The binding energies, hydrogen bonding, and Ki of all three sets of chemicals investigated are summarized in table. To anticipate the binding modes of the compounds, the criteria of lowest energy and maximum number of conformations per cluster were established.

The results from phytochemical screening for Psoriasis targets (IL-17 and IL-23):

Table 1: Results of drug and psoriatic targets receptor interaction

Plant name	**Major constitutes**	**Binding affinity to IL-17 (Kcal/Mol)**	**Binding affinity to IL-23 (Kcal/Mol)**
Coleus forskohlii	Forskolin	ΔG=−4.28 Ki=726.19 μm	ΔG=−4.70 Ki=357.28 μm
Rubia cordifolia	anthraquinones	ΔG=−6.28	ΔG=−6.90

		Ki=24.76 µm	Ki=8.78 µm
Azadirachta indica	Azadirachtin	ΔG=−2.32 Ki=19.79 mm	ΔG=−7.13 Ki=5.89 µm
Aloe barbadensis	Aloin	ΔG=−6.54 Ki=16.09 µm	ΔG=−6.08 Ki=35.01 µm
Boswellia serrata	11-keto-β-boswellic acid	ΔG=−8.46 Ki=632.75 nm	ΔG=−8.74 Ki=390.60 nm
Curcuma longa	Curcumin	ΔG=−7.22 Ki=5.11 µm	ΔG=−8.78 Ki=363.56 nm
Glycyrrhiza glabra	Glycyrrhizin	ΔG=−7.86 Ki=1.73 µm	ΔG=−6.92 Ki=8.51 µm
White willow bark	Salicin	ΔG=−6.46 Ki=18.39 µm	ΔG=−7.57 Ki=2.80 µm
Berberis aristata	Berberine	ΔG=−7.91 Ki=4.36 µm	ΔG=–8.44 Ki=653.28 nm

From above results, component berberine and 11-keto-β-boswellic acid shows maximum affinity to both proteins with ≅ −8 binding energy. Curcumin shows high affinity toward IL-23 with ΔG = −8.78, Ki = 363.56 nm than IL-17, and glycyrrhizin shows high affinity toward IL-17 with ΔG = −7.86, Ki = 1.73 µm than IL-23.

(1)

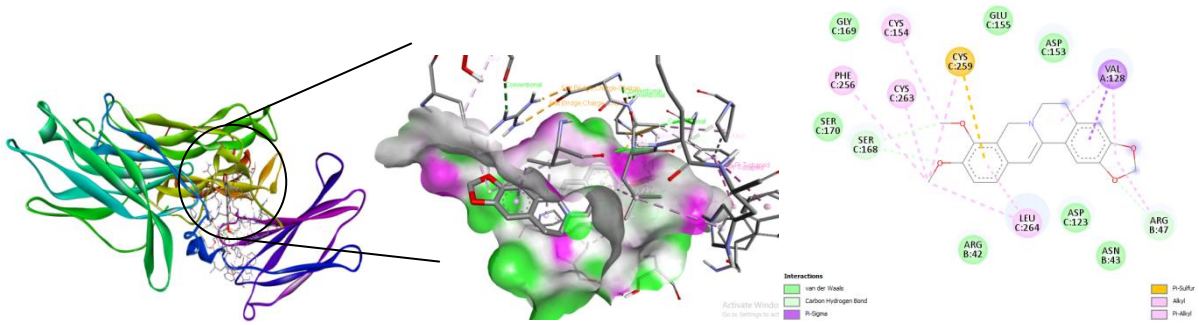

(a) **(b)** **(c)**

(2)

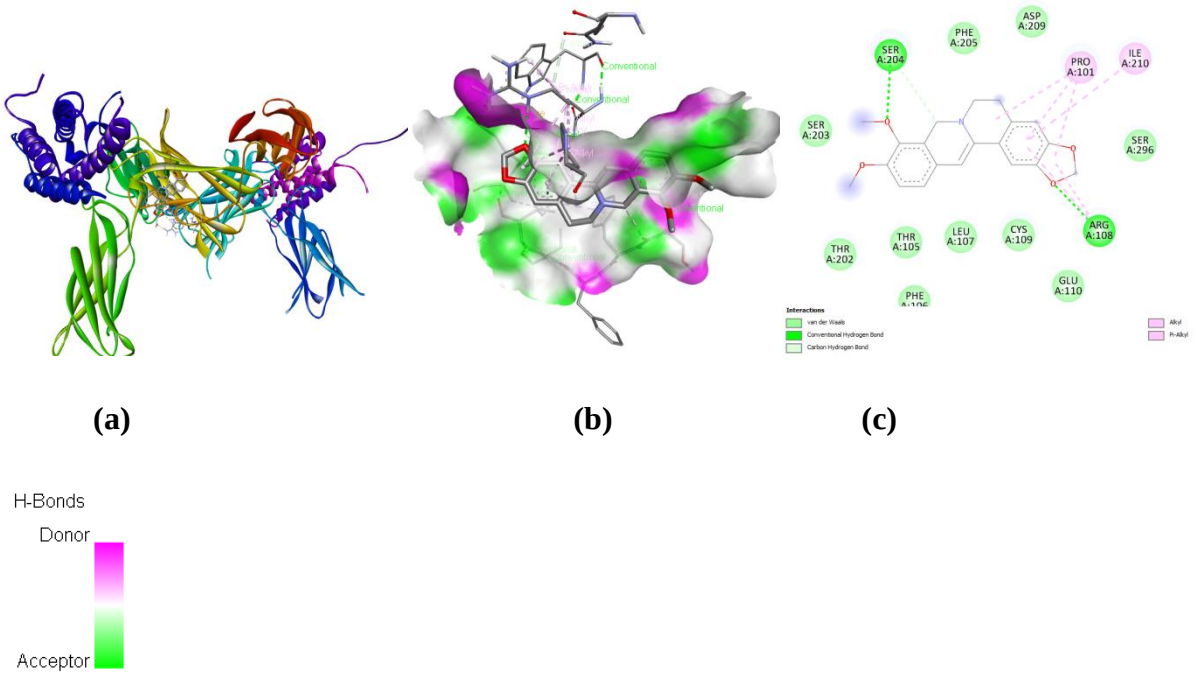

(a) **(b)** **(c)**

Figure 1: Visualization of the interaction between berberine and the IL-17(3JRF) receptor(**1**)and IL23(3DUH) receptor(**2**)demonstrating their strong affinity for one another

Berberin showed strong interaction with IL-17 by forming different types of bond interaction, such as GLY C:169, GLU C:155, ASP C:153, SER C:170, ARG B:42, ASP C:123, ASN B:43 involved in vaderwaals interaction, ARG B:47, SER C:168 involved in carbon hydrogen bond, and CYS C:259 involved in pi-sulfur interaction. THR A:202, LEU A:107, CYS A:109, GLU A:110, SER A:296, THR A:105, SER A:203, PHE A:205, ASP A:209 have been linked in vanderwaals intraction with IL-23 and ARG A:108, and SER A:204 shows conventional hydrogen bonds.

(3)

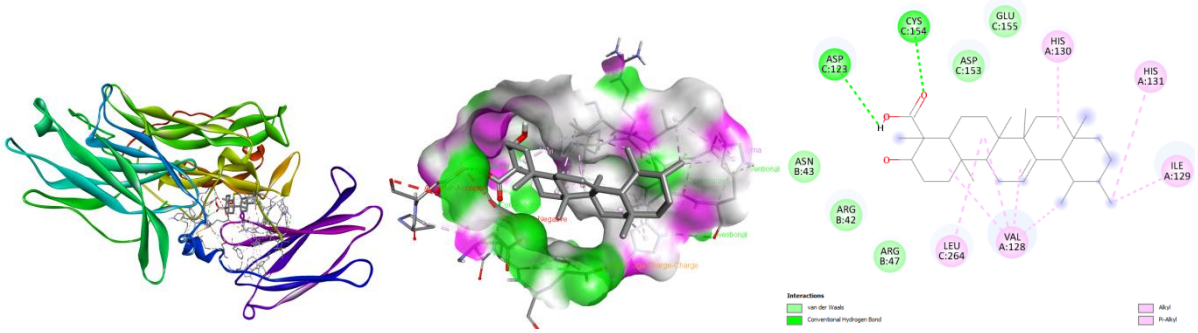

(a) **(b)** **(c)**

(4)

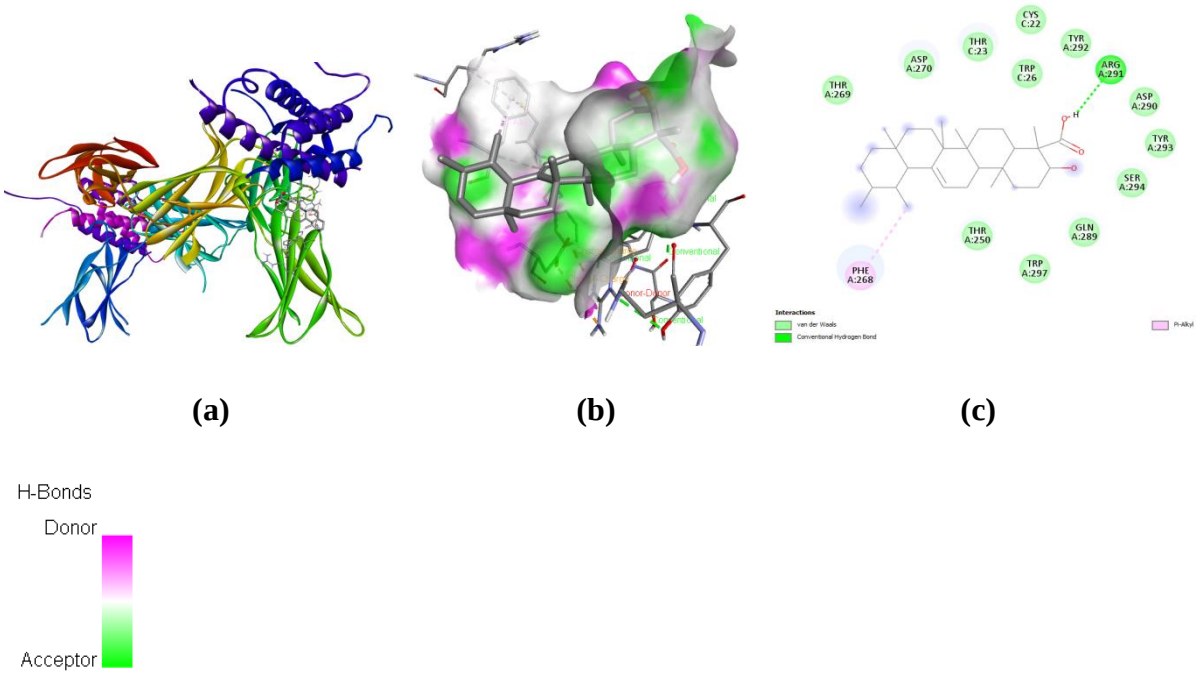

(a) **(b)** **(c)**

Figure 2: Visualization of the interaction between 11-keto-β-boswellic acid and the IL-17(3JRF) receptor(**3**) and IL23(3DUH) receptor(**4**) demonstrating their strong affinity for one another.

Docking and visualizing the outcomes11-keto-boswellic acid interacted strongly with IL-17 by establishing many types of bond interactions, such as: GLU C:155, ARG B:47, ARG B:42, ASP C:153, ASN B:43 engaged in vaderwaals contact, ASP C:123, CYS C:154 involved in carbon hydrogren bond, whereas HIS A:130:131, LEU C:264, VAL A:128, ILE A:129 involved in alkyl bond. THR A:269, THR A:250, THR C:23, CYS C:22, TYR A:292, ASP A:290, TYR A:293, SER A:293:294, GLN A:289, and TRP C:26 were implicated in vanderwaals interaction with IL-23.

Same process was repeated for inflammatory targets for screening of phytochemical. The results from phytochemical screening for inflammatory targets (COX-2 and TNF-α):

Table 2: Results of drug and inflammatory targets receptor interaction

Plant name	**Major constitutes**	**Binding affinity to TNF-α (Kcal/Mol)**	**Binding affinity to COX-2 (Kcal/Mol)**
Coleus forskohlii	Forskolin	ΔG=−4.67 Ki=378.21 µm	ΔG=−5.11 Ki=174.85 µm
Rubia cordifolia	Anthraquinones	ΔG=−6.86	ΔG=−8.00

		Ki=9.35 µm	Ki=1.37 µm
Azadirachta indica	Azadirachtin	ΔG=−6.31 Ki=23.83 µm	ΔG=−8.40 Ki=695.10 nm
Aloe barbadensis	Aloin	ΔG=−9.83 Ki=62.53 nm	ΔG=−7.93 Ki=1.55 nm
Boswellia serrata	11-keto-β-boswellic acid	ΔG=−9.86 Ki=58.99 nm	ΔG=−10.97 Ki=9.07 nm
Curcuma longa	curcumin	ΔG=−9.88 Ki=57.53 nm	ΔG=−8.65 Ki=458.35 nm
Glycyrrhiza glabra	glycyrrhizin	ΔG=−8.21 Ki=962.15 nm	ΔG=−10.21 Ki=32.68 nm
White willow bark	salicin	ΔG=−7.36 Ki=4.01 µm	ΔG=−7.15 Ki=5.70 µm
Berberis aristata	berberine	ΔG=−9.92 Ki=53.53 nm	ΔG=−10.32 Ki=27.21 nm

From ten compound, some compounds show good affinity toward TNF-α and some shows good affinity toward COX-2. Among chosen extracts berberine and 11-keto-β-boswellic acid shows maximum affinity to both inflammatory pathway targets and psoriatic targets. Curcumin had the high affinity for TNF- and COX-2, with ΔG = −9.88, Ki = 57.53nm and ΔG = −8.65, Ki = 458.35 nm, respectively. Whereas glycyrrhizin also had the high affinity for TNF- and COX-2, with ΔG = −8.21, Ki = 962.15 nm; ΔG= −10.21, Ki = 32.68 nm, respectively.

(5)

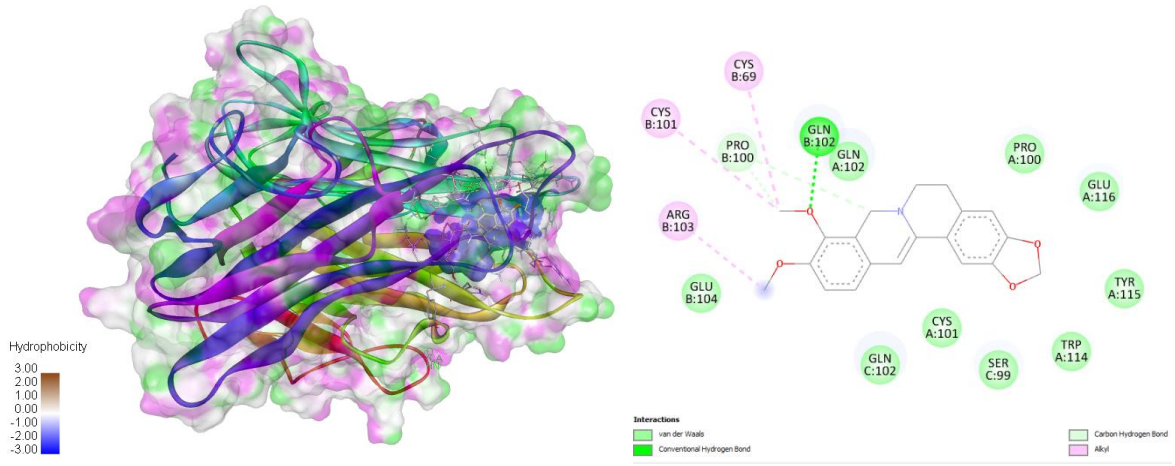

(a) **(b)**

(6)

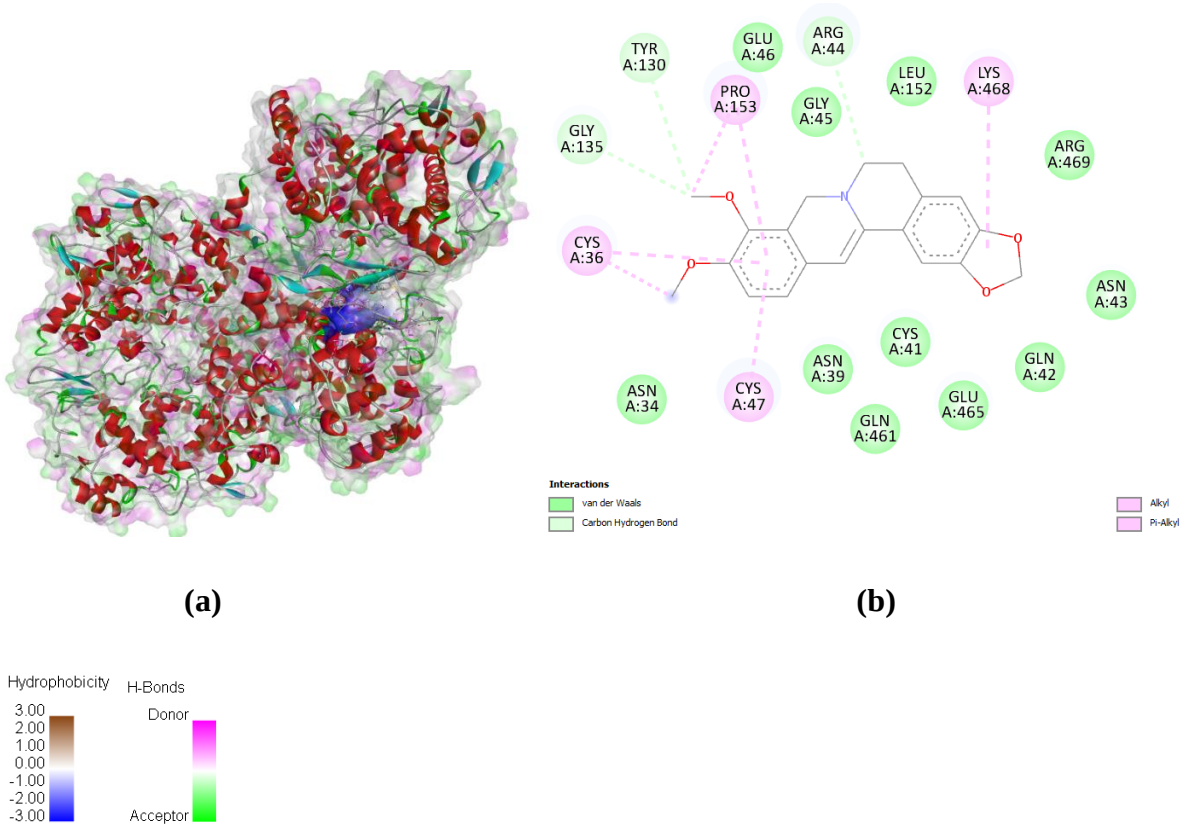

Figure 3: Visualization of the interaction between berberine and the TNF-α receptor (**5**) and COX-2 receptor (**6**) demonstrating their hydropathicity around ligands and H-bond donor and acceptor area along with 2-D representation of their interaction

Berberin interacted strongly with TNF- by forming various types of bond interactions, including GLN A:102, PRO A:100, GLU A:116, TYR A:115, TRP A:114, SER C:99, CYS A:101, GLN C:102, GLU B:104 involved in vaderwaals interaction, PRO B:100 involved in carbon hydrogrn bond, and GLN B:102 SHOW conventional hydrogen bond. GLU A:46, GLY A:45, LEU A:152, ARG A:469, ASN A:43, GLN A:42, GLU A:465, CYS A:41, ASN A:39 have been connected in vanderwaals interaction COX-2 and TYR A:130, ARG A:44, GLY A:135 associated with carbon hydrogen bond and CYS A:36, PRO A:153, LYS A:468, CYS A:47 exhibits alkyl bond.

(7)

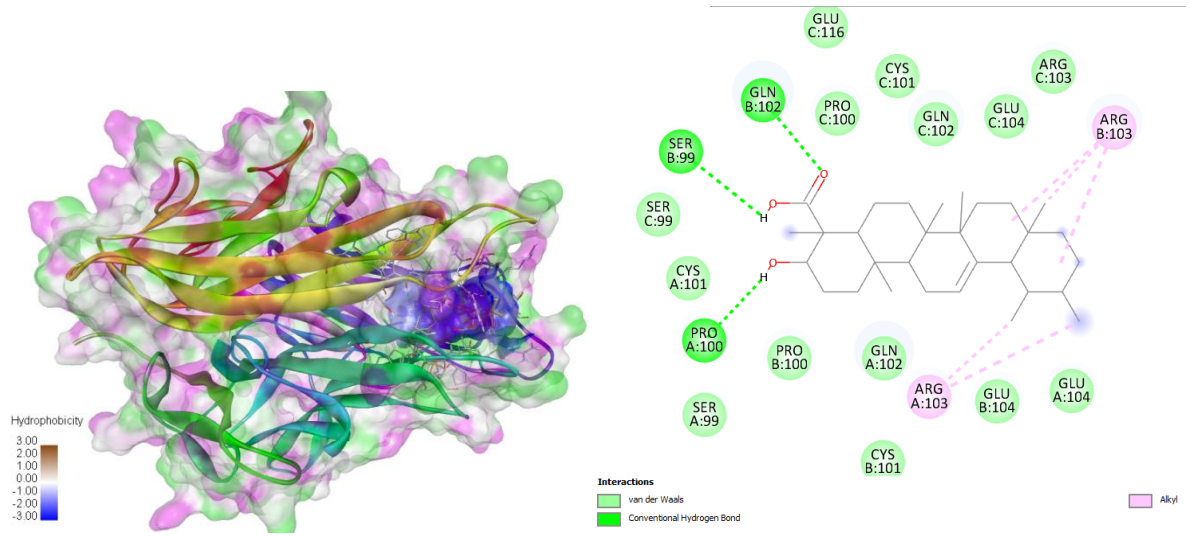

(a) **(b)**

(8)

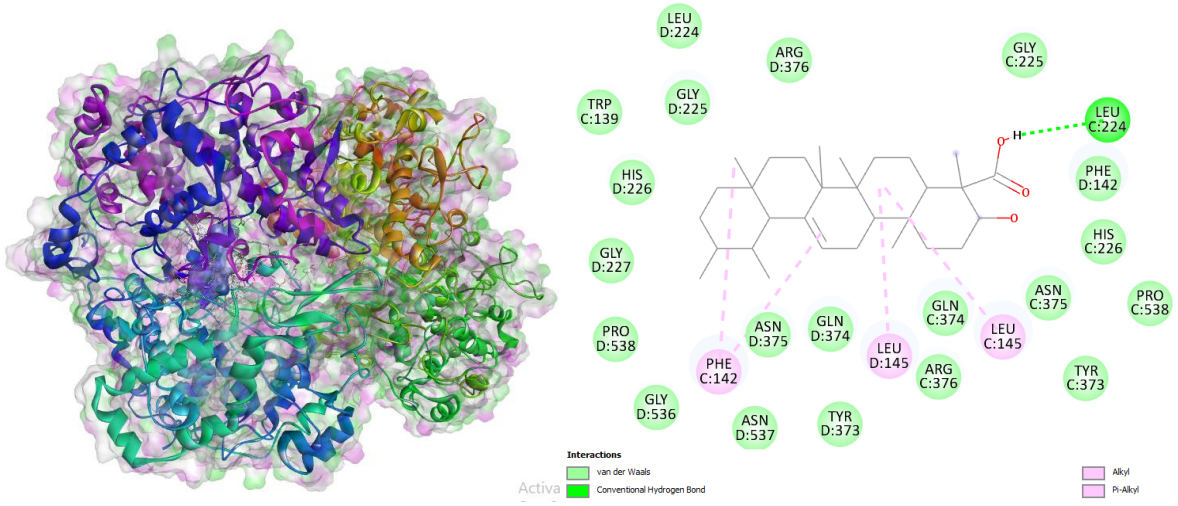

(a) **(b)**

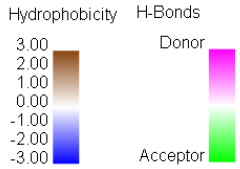

Figure 4: Visualization of the interaction between 11-keto-β-boswellic acid and the TNF-α receptor **(7a)** and COX-2 receptor (**8a**) demonstrating their hydropathicity around ligands and H-bond donor and acceptor area along with 2-D representation of their interaction. **(7b and 8b)** shows 2-D structure of interacting amino acid

By forming various types of bond interactions, such as the vaderwaals interaction involving

GLU C:116, PRO C:100, CYS C:101, GLN C:102, GLU C:104, ARG C:103, SER C:99, and the carbon hydrogen bond involving PRO A:100, GLN B:102, 11-keto-β-boswellic acid demonstrated strong interaction with TNF-. In vanderwaals interaction, COX-2 was coupled with LEU D:224, GLY D:225, ARG D:376, GLY C:225, PHE D:142, HIS C:226, PRO C:538, ASN C:375, GLN C:374, and GLY D:227. LEU D:224 was linked with a carbon hydrogen bond, while PHE C:142 and LEU D:145 showed an alkyl bond.

In first duration of work, retrieve 3D structure of protein from PDB and ligands structure from Pubchem and optimized it for docking purpose. All the previously mentioned herbal compounds were blindly docked against psoriatic and inflammatory targets and results were displayed in Tables 1 and 2, respectively. It generated ten clusters of confirmation of interaction, and the best confirmation was chosen based on their binding free energy (Gb, in kilocalories per mole) and inhibition constants, which were calculated with AutoDock 4.2. It can be well predicted from docking results that berberine (ΔG = −7.91, Ki = 4.36 μm against IL-17 and ΔG = −8.44, Ki = 653.28 nm for IL-23 for psoriatic targets while ΔG = −9.92, Ki = 53.53 nm for TNF-α and ΔG = −10.32, Ki = 27.21 nm for COX-2 for inflammatory targets) and 11-keto-β-boswellic acid ΔG = −8.46, Ki = 632.75 nm against IL-17 and ΔG = −8.74, Ki = 390.60 nm for IL-23 for psoriatic targets while ΔG = −9.86, Ki = 58.99 nm for TNF-α and ΔG = −10.97, Ki = 9.07 nm for COX-2 for inflammatory targets) both shows maximum affinity for all target proteins while some compounds like Curcumin had a high affinity for one of the psoriatic target proteins, IL-23, with a ΔG = −8.78, Ki = 363.56 nm, and glycyrrhizin has a high affinity for IL-17. Azadirachtin demonstrated a strong affinity for COX-2, an inflammatory target protein, with ΔG = −8.40, Ki = 695.10 nm. Aloin likewise demonstrated a higher affinity for TNF- than COX-2, with ΔG = −9.83, Ki = 62.53 nm.

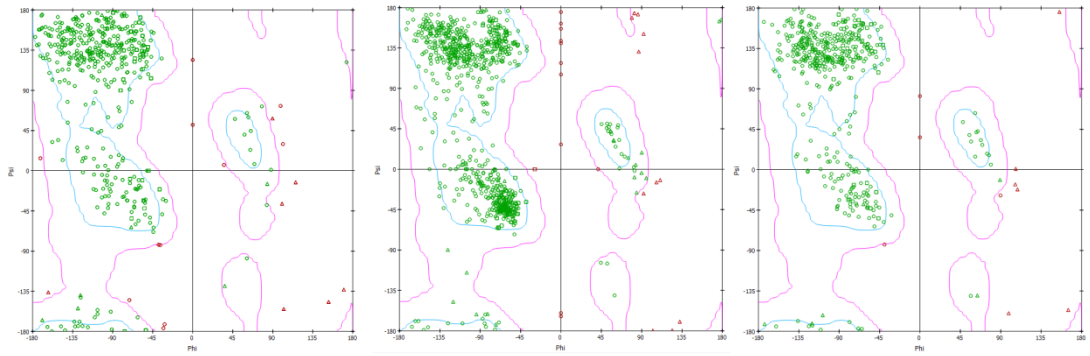

Berberine-IL-17 Berberine-IL-23 KBA-IL-17

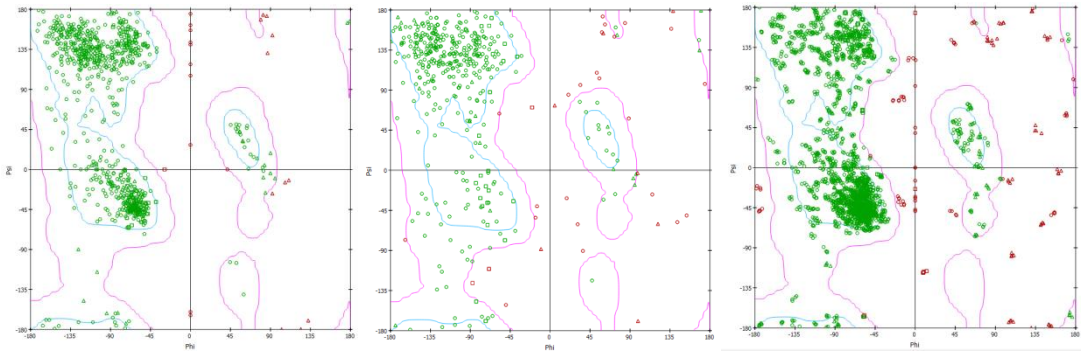

KBA-IL-23 Berberine-TNF-α Berberine-COX-2

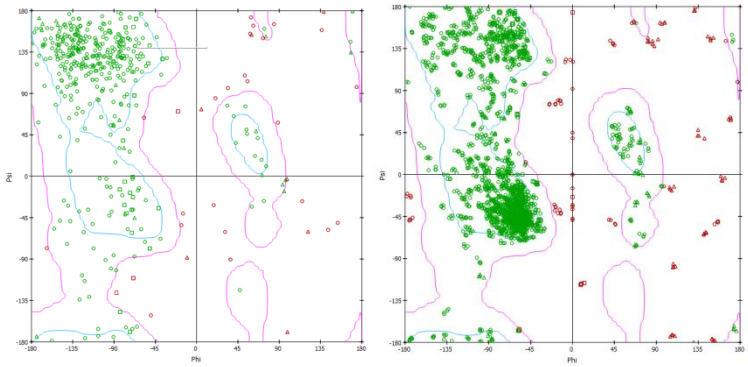

KBA-TNF-α KBA-COX-2

Figure 5: Ramachandran torsion plots of the eight complexes. The outlier residues have been marked in red

All of the structures were validated using the Ramachandran plot, as many of the residues in these eight complexes fell in the Ramachandran plot's preferred regions. There is no plot deviation. After validating all of the structures using the same method, only six compounds were chosen for further study: berberine, Azadirachtin, 11-keto--boswellic acid, curcumin, glycyrrhizin and Aloin as every constituents shows acceptable affinity either one of the protein from two pathway.

Ligand	Berberine	KBA	Azadirachtin	Curcumin	Glycyrrhizin	Aloin
AMES toxicity	Non-toxic	Non-toxic	Non-toxic	Non-toxic	Non-toxic	Toxic

According to the toxicity prediction, all constituents are non-toxic; however, Aloin exhibits some toxicity, thus we exclude that chemical from further research.

CONCLUSION

Computer-aided drug design allows for the evaluation of large chemical libraries in order to identify potential lead candidates that can be synthesized and tested. The *in silico* equivalent of high-throughput screening, virtual screening, holds immense potential for identifying novel medication candidates for the treatment of psoriasis.(Sree et.al 2022) we started with ten phytochemicals for *in silico* study and only five phytochemicals, berberine, Azadirachtin, 11-keto--boswellic acid, curcumin, and glycyrrhizin, demonstrated superior anti-inflammatory and anti-psoriatic capabilities.

REFERENCES

Anand, R., & Kaithwas, G. (2014). Anti-inflammatory potential of alpha-linolenic acid mediated through selective COX inhibition: computational and experimental data. *Inflammation*, *37*, 1297-1306.

Gudjonsson, J. E., Johnston, A., Sigmundsdottir, H., & Valdimarsson, H. (2004). Immunopathogenic mechanisms in psoriasis. *Clinical & Experimental Immunology*, *135*(1), 1-8.

Kamiya, K., Kishimoto, M., Sugai, J., Komine, M., & Ohtsuki, M. (2019). Risk factors for the development of psoriasis. *International Journal of Molecular Sciences*, *20*(18), 4347.

Prasanth, D. S. N. B. K., Murahari, M., Chandramohan, V., Panda, S. P., Atmakuri, L. R., & Guntupalli, C. (2021). In silico identification of potential inhibitors from Cinnamon against main protease and spike glycoprotein of SARS CoV-2. *Journal of Biomolecular Structure and Dynamics*, *39*(13), 4618-4632.

Qazi, S., & Raza, K. (2021). Phytochemicals from Ayurvedic plants as potential medicaments for ovarian cancer: an in silico analysis. *Journal of Molecular Modeling*, *27*, 1-14.

Rauf, M. A., Zubair, S., & Azhar, A. (2015). Ligand docking and binding site analysis with pymol and autodock/vina. *International Journal of Basic and Applied Sciences*, *4*(2), 168.

Saxena, S., Meher, K., Rotella, M., Vangala, S., Chandran, S., Malhotra, N.& Saxena, U. (2021). Identification of SGLT2 inhibitor Ertugliflozin as a treatment for COVID-19 using computational and experimental paradigm. *bioRxiv*, 2021-06. a

Saxena, S., Meher, K., Rotella, M., Vangala, S., Chandran, S., Malhotra, N., & Saxena, U. (2021). Tyrosine Kinase Inhibitor Family of Drugs as Prospective Targeted Therapy for

COVID-19 Based on in Silico And 3D-Human Vascular Lung Model Studies. *bioRxiv*, 2021-05. b

Sharmila, C. M., Devi, R. C., Sureka, A., MuthuKumar, N. J., & Banumathi, V. (2019). In silico analysis of the effect of vasicine and vasinone against human tyrosinase receptor in the management of hyperpigmentation of skin diseases. *Asian J. Pharm. Pharmacol*, *5*, 518-524.

Sravani, M., Kumaran, A., Dhamdhere, A. T., & Kumar, N. S. (2021). Computational molecular docking analysis and visualisation of anthocyanins for anticancer activity. *International Journal for Research in Applied Sciences and Biotechnology*, *8*(1), 154-161.

Sree, M. P., Yogan, G. P., & Gopal, V. (2022). Inhibitory Potentials of Phytoconstituents of Phyllanthus amarus against Severe Acute Respiratory Syndrome-Corona Virus-2 Main Protease: A Computational Aided Approach. *Indian Journal of Pharmaceutical Sciences*, *84*(5), 1203-1209.